IEEE Access
Multidisciplinary | Rapid Review | Open Access Journal

Received June 20, 2019, accepted July 1, 2019, date of publication August 5, 2019, date of current version August 16, 2019.

Digital Object Identifier 10.1109/ACCESS.2019.2933053

Design of a Microstrip Diplexer-Integrated Filtering Power Divider

CHI-FENG CHEN, (Member, IEEE), KAI-WEI ZHOU, RUEI-YI CHEN, ZU-CING WANG, AND YI-HUA HE

Department of Electrical Engineering, Tunghai University, Taichung 40704, Taiwan

Corresponding author: Chi-Feng Chen (cfchen@thu.edu.tw)

This work was supported by the Ministry of Science and Technology, Taiwan, under Grant MOST 107-2221-E-029-009 and Grant MOST 108-2221-E-029-001.

ABSTRACT This study proposed a new method and structure for designing a diplexer-integrated filtering power divider. A filtering function with equal power division was integrated with a diplexer. The multifunctional diplexer comprised eight coupled resonators and two 50-Ω resistors with a distributed coupling structure. Moreover, a connected coupling technique provided improved flexibility and freedom to construct the diplexer. High isolation was obtained using the proposed coupling configuration through the introduction of out-of-phase cancellation between multiple coupling routes. Moreover, because the distributed coupling structure was employed as an input, no complex matching network was required; this significantly reduced the size and simplified the design of the diplexer. Moreover, each channel passband was individually designed. For demonstration, a multifunctional diplexer operating at 1 and 1.15 GHz with a second-order Chebyshev bandpass response and equal power splitting was designed and fabricated using microstrip technology, and the simulation results were consistent with the measured results.

INDEX TERMS Bandpass filter (BPF), diplexer, microstrip, power divider (PD).

I. INTRODUCTION

Diplexers are crucial devices in multiservice and multiband microwave communication systems. Numerous high-performance diplexers have been studied [1]–[14]. A common resonator technique has been applied [1], [2], [5] to design diplexers. On the basis of this technique, the number of resonators can be reduced, without using any additional matching network. In [3], a diplexer was developed by integrating a dual-band bandpass filter (BPF) with two matching circuits. However, the size of the diplexer was relatively large. In [4], a diplexer was implemented using two slotline stepped-impedance resonator filters with a T-junction matching network. The T-junction matching network provided suitable transmission in one channel passband and appropriate attenuation in the other channel passband. In [6], a diplexer based on stub-loaded resonators with two independently controllable transmission zeros was proposed. These transmission zeros were properly located, and thus, the stopband rejection and isolation level of the diplexer were effectively elevated.

The associate editor coordinating the review of this manuscript and approving it for publication was Raghvendra Kumar Chaudhary.

In [7], a switchable function was integrated with a diplexer. P-i-n diodes were used and loaded at the end of the resonator to change resonance frequencies, and thus, each passband was turned on or off independently. In [8], a lowpass–bandpass diplexer was proposed. The matching circuit of the diplexer was within the BPF, thus reducing the size of the diplexer. In [9], a simple method was implemented to design balun diplexers by using two sets of open-loop ring resonators. In [10], inner-coupled dual-mode configurations were proposed and used to design a balanced diplexer. Moreover, two close differential-mode channels and suitable common-mode suppressions were successfully realized. In [11], second-order and fourth-order balanced-to-balanced diplexers based on magnetically coupled resonators were proposed. The two diplexers provided not only high-level isolation but also excellent differential-mode and common-mode performance. In [12], a diplexer formed using four pairs of asymmetric stepped impedance resonators (SIRs) with eight operation channels was developed for multiband communications. In [13], a diplexer with spiral-defected ground resonators was presented. Because of the slow-wave effect of a spiral-defected ground resonator, a broad out-of-band

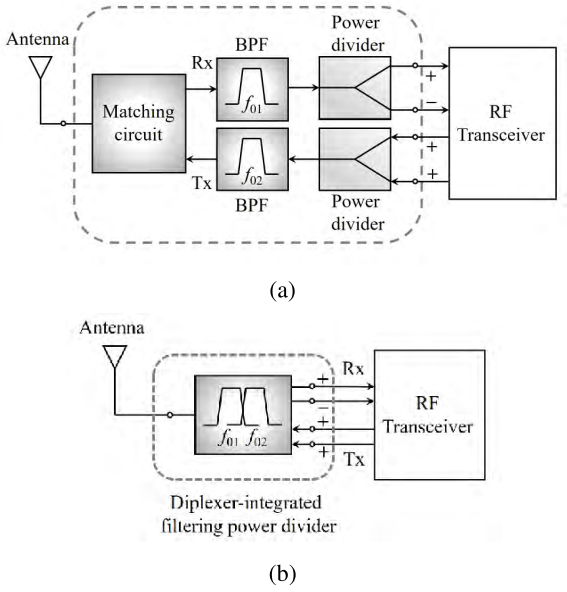

FIGURE 1. Block diagrams. (a) Cascaded connection of devices; (b) diplexer-integrated filtering PD.

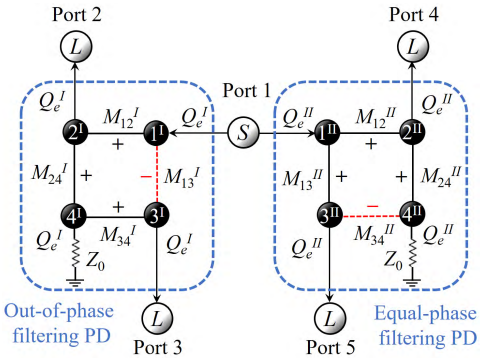

FIGURE 2. Coupling structure of the proposed diplexer-integrated filtering PD with second-order bandpass response.

characteristic was realized. Furthermore, a new design method was proposed for highly integrated multifunctional diplexers (i.e., multistate diplexers) [14]. The multiple frequency states of the diplexers were arbitrarily switched for implementing a frequency-hopping system.

With the rapid development of microwave communication technology, demands for multifunctional circuits are increasing. Studies have proposed different techniques for developing several power dividers (PDs) integrated with a BPF, which are termed filtering PDs [15]–[19]. On the basis of the coupled resonator technology, λ/4 lines of a conventional Wilkinson PD have been replaced with couplings of coupled resonators, thus providing PDs with a filtering function [15]–[17]. In [18] and [19], dual-mode filtering PDs have been proposed. Miniaturization was achieved for these PDs by using one or two dual-mode resonators. Furthermore, to yield duplexing power division and filtering function for applications in dual-band front-end systems, the cascaded connection of a matching circuit, two BPFs, and two PDs were used [Fig. 1(a)]; however, this implementation increased the circuit area and power loss. The aforementioned limitations can be effectively overcome by integrating these devices into a single multifunctional component (i.e., a diplexer-integrated filtering PD) [Fig. 1(b)]. Few studies have investigated diplexer-integrated filtering PDs [20]–[22].

This study proposed a new method for designing a diplexer-integrated filtering PD based on coupled resonators. The selection of suitable coupling coefficients of resonators and external quality factors of input/output (I/O) resonators can not only facilitate filtering and power division functions but also provide an appropriate isolation over operating bands. To validate the aforementioned statement, a diplexer-integrated filtering PD operating at 1 and 1.15 GHz was designed and fabricated. The fabricated circuit had equal-phase and out-of-phase power divisions. The equal-phase PD of a transmitter (Tx) was used for combining power, whereas the out-of-phase PD was used for a balanced receiver (Rx) design for practical applications. This design was validated through full-wave simulation and measured results. Compared with other state-of-art multifunctional diplexers, the proposed diplexer exhibits advantages such as simple layout, compact size, low loss, and high isolation.

The remainder of this paper is organized as follows: Section 2 presents the detailed procedure for designing the proposed diplexer-integrated filtering PD. In Section 3, a diplexer-integrated filtering PD was implemented using microstrip technology for a demonstration. The experimental results were presented and compared with full-wave electromagnetic simulated results. Furthermore, the results were compared with previous state-of-art multifunctional diplexers, and the advantages of the proposed diplexer were highlighted. Finally, Section 4 presents the conclusion.

II. CIRCUIT DESIGN

Fig. 2 shows the coupling structure of the proposed diplexer-integrated filtering PD, where each node represents a resonator, and S and L are a source and load, respectively. A second-order Chebyshev filtering function with equal power splitting was integrated into the diplexer. Port 1 was an input port and ports 2–5 were output ports. The multifunctional diplexer was a combination of equal-phase and out-of-phase filtering PDs operating at different frequency bands. The passbands of channels I and II were formed using resonators $1^{\mathrm{I}} - 4^{\mathrm{I}}$ and $1^{\mathrm{II}} - 4^{\mathrm{II}}$, respectively. To improve in-band isolation, coupling routes denoted with dashed lines were out of phase with the other routes; that is, the sign of the corresponding coupling coefficient was negative, which was in contrast to those of other coupling coefficients. When one of the output ports of a filtering PD was excited, the other output port received an equal amount of power with a reverse phase. Therefore, no coupling was observed between the output ports of any channel. The required coupling coefficients and external quality factors of a multifunctional diplexer are

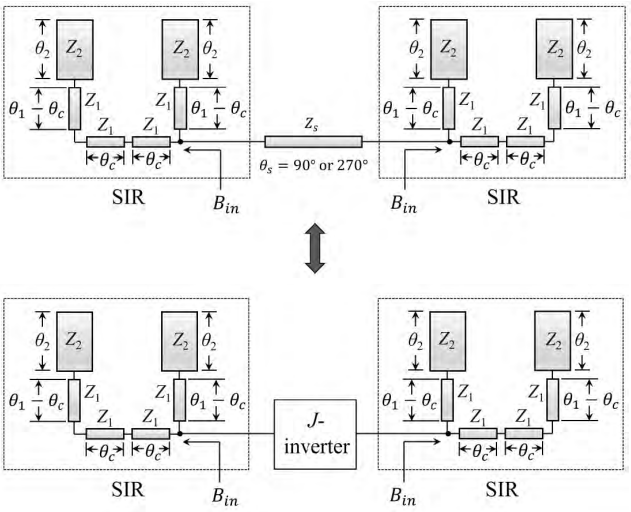

FIGURE 3. Equivalent circuits of the coupling scheme.

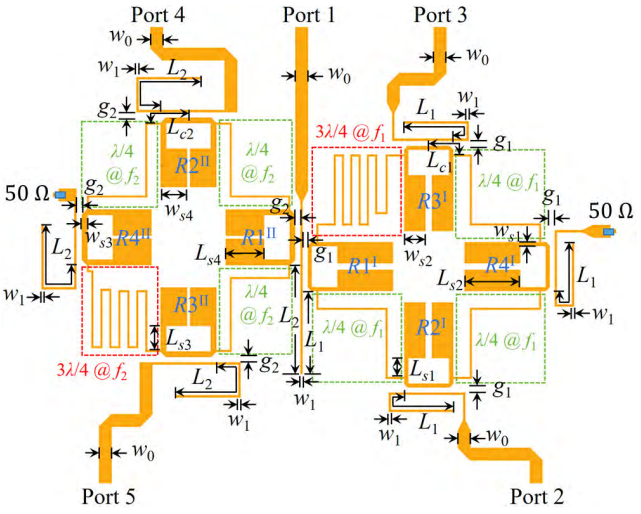

FIGURE 4. Microstrip configuration of the proposed diplexer-integrated filtering PD.

as follows:

$$M_{12}^{I} = -M_{13}^{I} = M_{24}^{I} = M_{34}^{I} = \frac{1}{\sqrt{2}} \cdot \frac{\Delta^{I}}{\sqrt{g_1 g_2}} \tag{1}$$

$$M_{12}^{II} = M_{13}^{II} = M_{24}^{II} = -M_{34}^{II} = \frac{1}{\sqrt{2}} \cdot \frac{\Delta^{II}}{\sqrt{g_1 g_2}} \tag{2}$$

and

$$Q_e^n = \frac{g_0 g_1}{\Delta^n}, \quad n = \mathrm{I}, \mathrm{II} \tag{3}$$

where g-values and Δ denote lumped element values of a low-pass prototype filter and fractional bandwidth, respectively. When a passband ripple of 0.04321 dB was selected, the corresponding lumped element values are as follows: $g_0 = 1$, $g_1 = 0.6648$, and $g_2 = 0.5445$ [23].

Conventional coupling structures, such as parallel-coupled lines and capacitive-coupled configurations, have some limitations, particularly in terms of circuit layouts. For example, to realize gap coupling through the close placement of coupled-line sections of the two resonators, the distance between the coupled resonators must be small. The implementation of the proposed coupling structure (Fig. 2) by using a general coupled resonator pair, such as hairpin resonators and SIRs, with conventional gap coupling was difficult. Therefore, a connected coupling technique with a flexible structure was introduced for this design [24]. Fig. 3 shows the equivalent circuit of the connected coupling scheme, where a pair of SIRs was coupled using an admittance inverter (J-inverter). In [25], a $\lambda/4$ or $3\lambda/4$ transformer with an appropriate characteristic impedance(Z_s) was modeled as an admittance inverter. Therefore, a connected coupling scheme can be used. In the proposed design, input susceptance B_{in} into the connecting point was as follows:

$$B_{in} = \mathrm{Im}\left[j\frac{Z_1 \tan\theta_2 + Z_2 \tan(\theta_1 - \theta_c)}{Z_1 Z_2 - Z_1^2 \tan\theta_2 \tan(\theta_1 - \theta_c)} - \frac{j}{Z_1 \tan\theta_c} \right] \tag{4}$$

TABLE 1. Circuit specification.

	Channel I	Channel II
Central frequency (GHz)	1	1.15
Fractional bandwidth (%)	3.5	3.6
Filter order	2	2
Response	Chebyshev (0.04321 dB ripple)	

The corresponding susceptance slope parameter b of the resonator at central frequency ω_0 is as follows:

$$b = \frac{\omega_0}{2} \frac{\partial B_{in}}{\partial \omega_0}\bigg|_{\omega_0} \tag{5}$$

The coupling coefficient between resonators i and $i+1$ is as follows:

$$M_{i,i+1} = \frac{J_{i,i+1}}{\sqrt{b_i b_{i+1}}} \tag{6}$$

where b_i and b_{i+1} are the susceptance slope parameters of resonators i and $i+1$, respectively, whereas $J_{i,i+1}$ is the inverter value. Therefore, the coupling coefficient could be controlled by changing the feeding position of the connecting line on coupled resonators (i.e., θ_c). Because $\lambda/4$ and $3\lambda/4$ connected couplings had a phase difference of 180°, these couplings had opposite signs. Thus, positive couplings, namely M_{12}^{I}, M_{24}^{I}, M_{34}^{I}, M_{12}^{II}, M_{13}^{II}, and M_{24}^{II}, and negative couplings, namely M_{13}^{I} and M_{34}^{II}, were implemented using $\lambda/4$ and $3\lambda/4$ connected couplings, respectively.

For demonstration, a diplexer-integrated filtering PD was designed using microstrip technology and implemented on a Rogers RO4003 substrate with a relative dielectric constant and thickness of 3.38 and 1.524 mm, respectively, to fit the specifications (Table 1). Fig. 4 shows the circuit layout of the proposed multifunctional microstrip diplexer. In this design, all resonators were realized using SIRs. Resonators 1^{I}–4^{I} and

TABLE 2. Design parameters of resonators.

Resonator	Z_1 (Ω)	Z_2 (Ω)	θ_1 (°)	θ_2 (°)
$1^{\mathrm{I}} - 4^{\mathrm{I}}$	96	35	26.2	29.5
$1^{\mathrm{II}} - 4^{\mathrm{II}}$	80	30	32.3	23.4

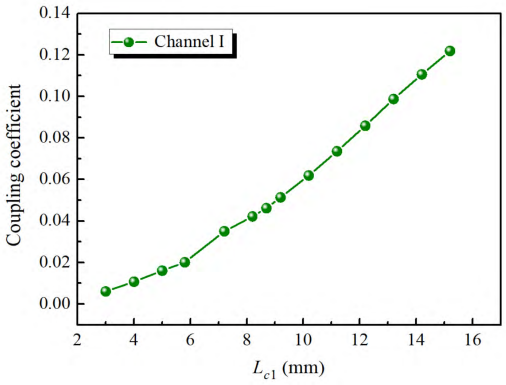

(a)

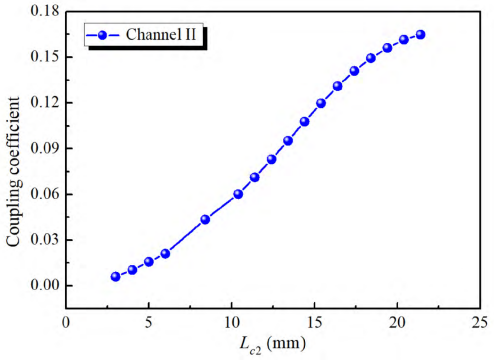

(b)

FIGURE 5. Design curves for coupling coefficient. (a) Channel I and (b) Channel II. ($Z_s = 132$ Ω)

$1^{\mathrm{II}} - 4^{\mathrm{II}}$ were designed with frequencies of 1 and 1.15 GHz, respectively. Table 2 presents the design parameters of these SIRs. The circuit layout was simple and flexible by using connected couplings. Because of miniaturization considerations, a compact-sized layout was designed by bending all connecting lines and SIRs. According to the provided specification, the required coupling coefficients and external quality factors were calculated using (1)–(3) as follows: $M_{12}^{I} = -M_{13}^{I} = M_{24}^{I} = M_{34}^{I} = 0.041$, $M_{12}^{II} = M_{13}^{II} = M_{24}^{II} = -M_{34}^{II} = 0.042$, $Q_e^{I} = 18.99$, and $Q_e^{II} = 18.47$.

As mentioned previously, coupling strength between resonators was controlled by appropriately adjusting the feeding position of the connecting lines on coupled resonators, namely L_{c1} and L_{c2} (Fig. 4). Coupling coefficient M_{ij} between resonators i and j is evaluated using the following formula [23]:

$$M_{ij} = \pm \frac{f_{p2}^2 - f_{p1}^2}{f_{p2}^2 + f_{p1}^2} \tag{7}$$

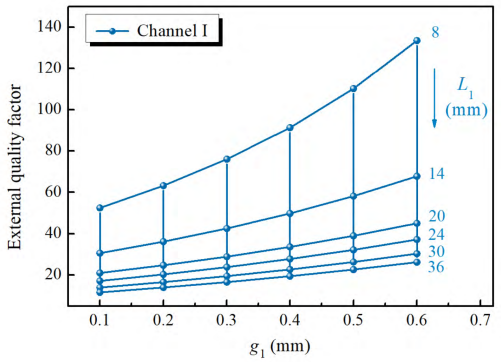

(a)

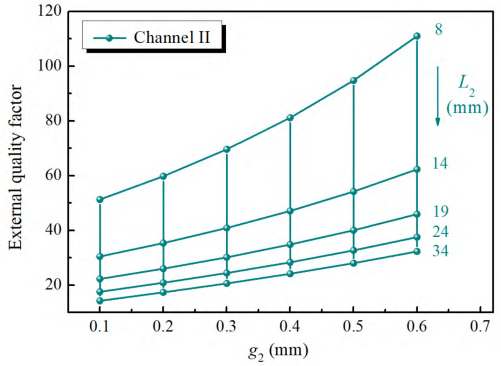

(b)

FIGURE 6. Design curves for Q_e. (a) Channel I and (b) Channel II. ($w_1 = 0.5$ mm)

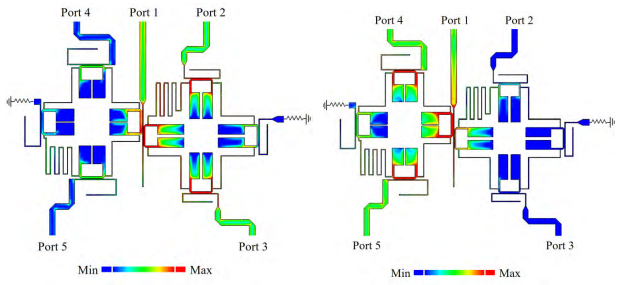

(a) (b)

FIGURE 7. Current distribution of the proposed diplexer-integrated filtering PD. (a) 1 GHz and (b) 1.15 GHz.

where f_{p1} and f_{p2} are lower and higher fundamental resonant frequencies of two coupled resonators under weak coupling, respectively. Figs. 5(a) and 5(b) illustrate the variation in the extracted coupling coefficients with respect to different values of L_{c1} and L_{c2}, respectively.

External quality factors could be controlled by appropriately adjusting the geometric parameters w_1, L_1, g_1, L_2, and g_2 of an I/O coupling structure. The external quality factor is evaluated using the I/O resonator and following equation [23]:

$$Q_e = \frac{\pi f_0 \tau_d\,(f_0)}{2} \tag{8}$$

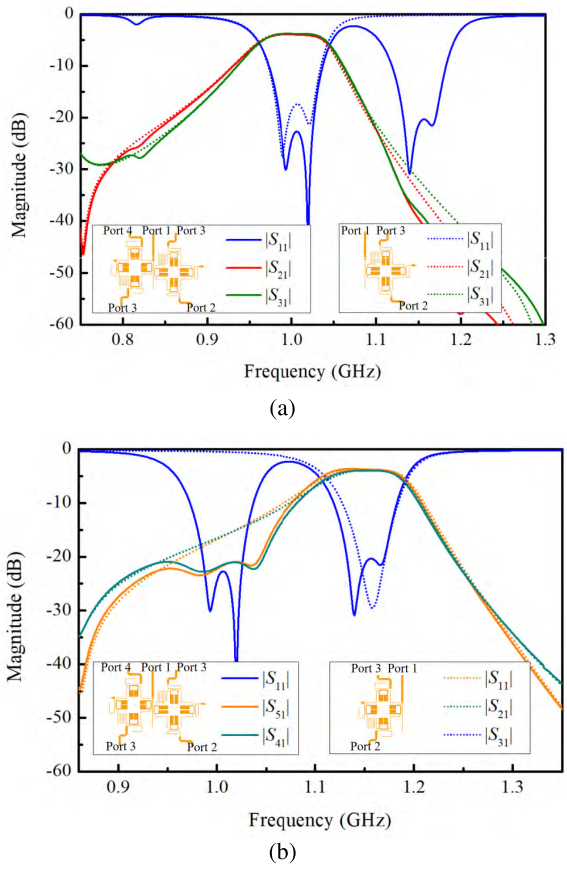

FIGURE 8. Simulated S-parameters. (a) 1 GHz filtering PD and diplexer-integrated filtering PD; (b) 1.15 GHz filtering PD and diplexer-integrated filtering PD.

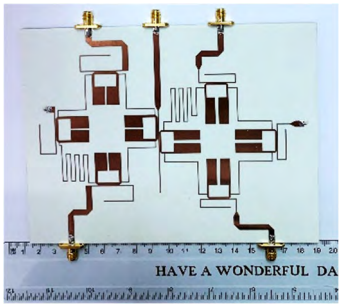

FIGURE 9. Picture of the fabricated diplexer-integrated filtering PD.

where τ_d (f_0) denotes group delay at central frequency f_0. Figs. 6(a) and 6(b) show the design curves of the extracted Q_e^I and Q_e^{II}, respectively. The structural parameters of the multifunctional diplexer were determined when the extracted values of coupling coefficients and external quality factors corresponded to the theoretical values.

A distributed coupling structure was employed to integrate the two filtering PDs. For compactness, the 1-GHz out-of-phase and 1.15-GHz equal-phase filtering PDs were placed on the left and right sides of input coupled lines,

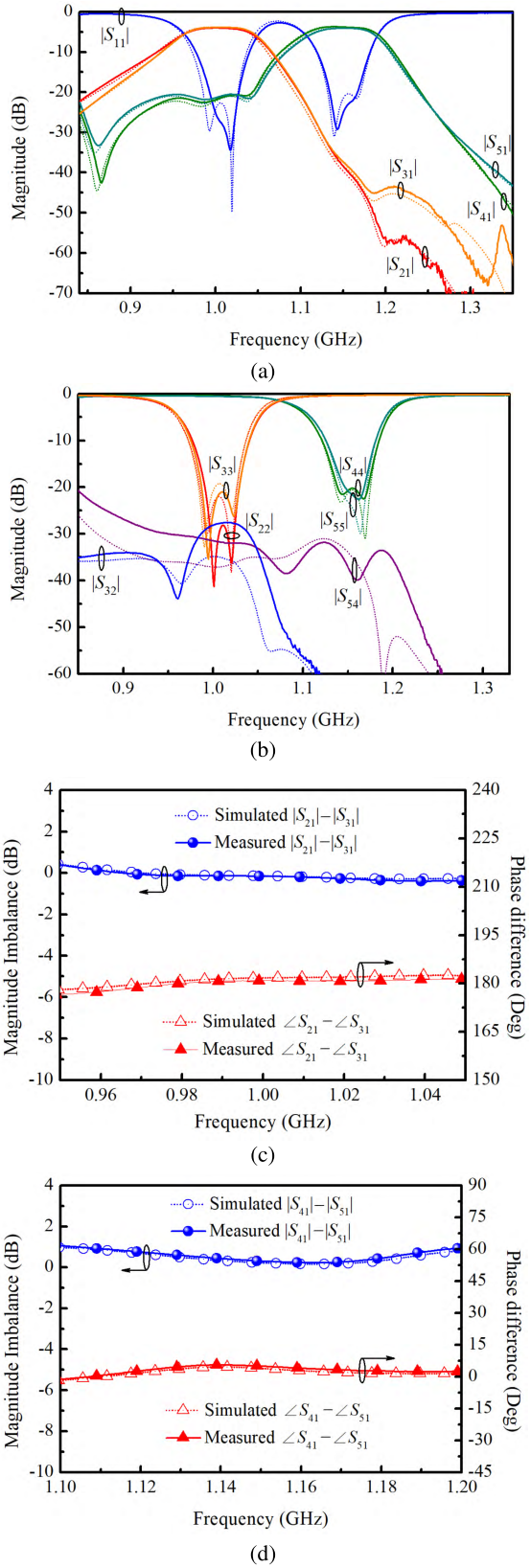

FIGURE 10. Simulation and measurement. (a) $|S_{11}|$, $|S_{21}|$, $|S_{31}|$, $|S_{41}|$, and $|S_{51}|$; (b) $|S_{22}|$, $|S_{33}|$, $|S_{44}|$, $|S_{55}|$, $|S_{32}|$, and $|S_{54}|$; (c) $|S_{21}|-|S_{31}|$ and $<S_{21}-<S_{31}$; (d) $|S_{41}|-|S_{51}|$ and $<S_{41}-<S_{51}$. (solid line: measurement, dashed line: simulation).

TABLE 3. Comparison with other previous works.

	Central frequency (GHz)	Central frequency ratio	Fractional bandwidth (%)	In-band insertion loss (dB)	Isolation (dB)	Size (λ_g^2)	Power dividing function
This work	1, 1.15	1.15	3.5, 3.6	0.7, 0.8	> 28, > 35	0.26	Yes
[5]	1.95, 2.14	1.1	3.6, 3.3	1.2, 1.5	40, 35	0.14	No
[9]	2.59, 5.41	2.09	9.26, 5.73	2.73, 3.68	> 35	0.18	Yes
[13]	1.78, 2.4	1.35	9.6, 10.8	1.59, 1.59	> 30	0.043	No
[20]	28.2, 29.2	1.04	2.3, 2.2	0.9, 0.8	N.A.	N.A.	Yes
[21] Case 1	1.77, 2.38	1.34	N.A.	0.74, 0.95	39, 31	> 0.3	Yes
[21] Case 2	1.78, 2.35	1.32	N.A.	0.45, 0.77	28, 35	> 0.3	Yes
[21] Case 3	1.75, 2.4	1.37	N.A.	0.5, 0.74	30, 32	> 0.3	Yes
[22]	2.5, 3	1.2	N.A.	1.6, 1.9	> 27, > 21	0.2	Yes

respectively. Because the distributed coupling structure providing a low loading effect was adopted in this design, 1- and 1.15-GHz filtering PDs were individually designed before integrating to form a multifunctional diplexer. Moreover, no additional matching network was required for this design, thus reducing the size of the diplexer. Figs. 7(a) and (b) show the current distributions of the proposed diplexer-integrated filtering PD at 1 and 1.15 GHz, respectively. The 1- and 1.15-GHz electromagnetic (EM) waves were transmitted from input to outputs through different paths. Furthermore, Figs. 8(a) and (b) show the EM simulated results of a single 1- or 1.15-GHz filtering PD and diplexer-integrated filtering PD. The in-band transmission coefficients were approximately the same when another filtering PD was included to the existing filtering PD for forming a diplexer-integrated filtering PD, which validated the low-loading effect of the distributed coupling structure. The aforementioned loading effect analysis indicated that each channel passband of the diplexer-integrated filtering PD could be independently implemented.

III. EXPERIMENT AND MEASUREMENT

The obtained parameters satisfying the required specification are as follows: $w_0 = 3.54$ mm, $w_1 = 0.5$ mm, $w_{s1} = 1$ mm, $w_{s2} = 6$ mm, $w_{s3} = 1.5$ mm, $w_{s4} = 7.5$ mm, $L_{s1} = 5.6$ mm, $L_{s2} = 16$ mm, $L_{s3} = 7.1$ mm, $L_{s4} = 11$ mm, $L_1 = 24$ mm, $L_2 = 31.5$ mm, $L_{c1} = 8.5$ mm, $L_{c2} = 8$ mm, $g_1 = 0.13$ mm, and $g_2 = 0.15$ mm. The diplexer-integrated filtering PD had an overall circuit area of $0.67\lambda_g \times 0.39\lambda_g$ (i.e., 132.1×78 mm^2). Fig. 9 shows a picture of the fabricated diplexer-integrated filtering PD.

Figs. 10(a)–(d) present the simulated and measured performance of the proposed multifunctional diplexer. The measurement results were obtained using a two-port Agilent N5230A vector network analyzer, whereas full-wave EM simulation results were obtained using an Advanced Design System by Agilent Technologies. A second-order filtering response with equal power splitting was successfully obtained. The measured return losses (i.e., $-20\log|S_{11}|$) were higher than 20 dB for both the channel passbands. Furthermore, the measured insertion losses (i.e., $-20\log|S_{21}|$ or $-20\log|S_{31}|$ and $-20\log|S_{41}|$ or $-20\log|S_{51}|$) were approximately $(3+0.7)$ and $(3+0.8)$ dB for channels I and II, respectively, where the 3-dB is due to the power dividing loss of output ports. The measured isolations ($-20\log|S_{32}|$ and $-20\log|S_{54}|$) were higher than 28 and 35 dB over the complete passbands at lower and higher channels, respectively. Moreover, within the operating passbands, the measured phase differences $\angle S_{21} - \angle S_{31}$ and $\angle S_{41} - \angle S_{51}$ were between $180° \pm 4.1°$ and between $0° \pm 5.5°$, respectively. The measured magnitude imbalances $|S_{21}| - |S_{31}|$ and $|S_{41}| - |S_{51}|$ were within 0.4 and 0.9 dB, respectively.

Table 3 compares the results of the proposed design with the previous state-of-art multifunctional diplexers. The proposed circuit was smaller and had a simpler layout than the duplexing PDs in [20] and [21]. Furthermore, the in-band isolation of the duplexing PDs in [21] was not satisfactory. The experimental results indicated that satisfactory isolation was only achieved around the central frequency, whereas isolation was unsatisfactory at the edge of the passband. Although the integrated diplexer-PD in [22] is advantageous because of its compact size, using multimode resonators increases design complexity. Moreover, such a circuit structure requires four via holes for practical implementation, thus increasing fabrication complexity.

IV. CONCLUSION

In this study, a microstrip diplexer-integrated filtering PD was developed. This multifunctional diplexer can replace several cascaded circuits to reduce power loss and circuit area. The design was successfully validated through an EM simulation and measured results. The proposed multifunctional diplexer is advantageous for practical applications in modern communication systems because of its simple layout, compact size, low loss, and high isolation.

REFERENCES

[1] C.-F. Chen, T.-Y. Huang, C.-P. Chou, and R.-B. Wu, "Microstrip diplexers design with common resonator sections for compact size, but high isolation," *IEEE Trans. Microw. Theory Techn.*, vol. 54, no. 5, pp. 1945–1952, May 2006.
[2] M.-L. Chuang and M.-T. Wu, "Microstrip diplexer design using common T-shaped resonator," *IEEE Microw. Wireless Compon. Lett.*, vol. 21, no. 11, pp. 583–585, Nov. 2011.
[3] P.-H. Deng, C.-H. Wang, and C. H. Chen, "Compact microstrip diplexers based on a dual-passband filter," in *Asia–Pacific Microw. Conf. Dig.*, Dec. 2006, pp. 1228–1232.
[4] H. Liu, W. Xu, Z. Zhang, and X. Guan, "Compact diplexer using slotline stepped impedance resonator," *IEEE Microw. Wireless Compon. Lett.*, vol. 23, no. 2, pp. 75–77, Feb. 2013.
[5] X. Guan, F. Yang, H. Liu, and L. Zhu, "Compact and high-isolation diplexer using dual-mode stub-loaded resonators," *IEEE Microw. Wireless Compon. Lett.*, vol. 24, no. 6, pp. 385–387, Jun. 2014.
[6] C. F. Chen, C. Y. Lin, B. H. Tseng, and S. F. Chang, "High-isolation and high-rejection microstrip diplexer with independently controllable transmission zeros," *IEEE Microw. Wireless Compon. Lett.*, vol. 24, no. 12, pp. 851–853, Dec. 2014.
[7] S.-C. Weng, K.-W. Hsu, and W.-H. Tu, "Switchable and high-isolation diplexer with wide stopband," *IEEE Microw. Wireless Compon. Lett.*, vol. 24, no. 6, pp. 373–375, Jun. 2014.
[8] P.-H. Deng, R.-C. Liu, W.-D. Lin, and W. Lo, "Design of a microstrip low-pass-bandpass diplexer using direct-feed coupled-resonator filter," *IEEE Microw. Wireless Compon. Lett.*, vol. 27, no. 3, pp. 254–256, Mar. 2017.
[9] C.-M. Chen, S.-J. Chang, C.-F. Yang, and C.-Y. Chen, "A simple and effective method for designing frequency adjustable balun diplexer with high common-mode suppression," *IEEE Microw. Wireless Compon. Lett.*, vol. 25, no. 7, pp. 433–435, Jul. 2015.
[10] X. Guo, L. Zhu, and W. Wu, "Balanced Diplexers based on inner-coupled dual-mode structures with intrinsic common-mode suppression," *IEEE Access*, vol. 5, pp. 26774–26782, 2017.
[11] A. Fernández-Prieto, A. Lujambio, J. Martel, F. Medina, F. Martin, and R. R. Boix, "Balanced-to-balanced microstrip diplexer based on magnetically coupled resonators," *IEEE Access*, vol. 6, pp. 18536–18547, 2018.
[12] Y.-W. Chen, H.-W. Wu, C.-T. Chiu, and Y.-K. Su, "Design of new eight-channel diplexer for multiband wireless communication system," *IEEE Access*, vol. 6, pp. 49732–49739, 2018.
[13] K. Song, Y. Zhou, Y. Chen, S. R. Patience, S. Guo, and Y. Fan, "Compact high-isolation multiplexer with wide stopband using spiral defected ground resonator," *IEEE Access*, vol. 7, pp. 31702–31710, 2019.
[14] Z.-C. Zhang, S.-W. Wong, J.-Y. Lin, H. Liu, L. Zhu, and Y. He, "Design of multistate diplexers on uniform- and stepped-impedance stub-loaded resonators," *IEEE Trans. Microw. Theory Techn.*, vol. 67, no. 4, pp. 1452–1460, Apr. 2019.
[15] J.-Y. Shao, S.-C. Huang, and Y.-H. Pang, "Wilkinson power divider incorporating quasi-elliptic filters for improved out-of-band rejection," *Electron. Lett.*, vol. 47, no. 23, pp. 1288–1289, Nov. 2011.
[16] C.-F. Chen, T.-Y. Huang, T.-M. Shen, and R.-B. Wu, "Design of miniaturized filtering power dividers for system-in-a-package," *IEEE Compon., Packag., Manuf. Technol.*, vol. 3, no. 10, pp. 1663–1672, Oct. 2013.
[17] C.-F. Chen and C.-Y. Lin, "Compact microstrip filtering power dividers with good in-band isolation performance," *IEEE Microw. Wireless Compon. Lett.*, vol. 24, no. 1, pp. 17–19, Jan. 2014.
[18] G. Zhang, J. Wang, L. Zhu, and W. Wu, "Dual-mode filtering power divider with high passband selectivity and wide upper stopband," *IEEE Microw. Wireless Compon. Lett.*, vol. 27, no. 7, pp. 642–644, Jul. 2017.
[19] G. Zhang, X. D. Wang, J.-S. Hong, and J. Q. Yang, "A high-performance dual-mode filtering power divider with simple layout," *IEEE Microw. Wireless Compon. Lett.*, vol. 28, no. 2, pp. 120–122, Feb. 2018.
[20] M. S. Sorkherizi, A. Vosoogh, A. A. Kishk, and P.-S. Kildal, "Design of integrated diplexer-power divider," in *IEEE MTT-S Int. Microw. Symp. Dig.*, May 2016, pp. 1–3.
[21] P.-H. Deng, W. Lo, B.-L. Chen, and C.-H. Lin, "Designs of diplexing power dividers," *IEEE Access*, vol. 6, pp. 3872–3881, 2018.
[22] G. Zhang, Z. Qian, and J. Yang, "Design of a compact microstrip power-divider diplexer with simple layout," *Electron. Lett.*, vol. 54, no. 16, pp. 1007–1009, Aug. 2018.
[23] J. S. Hong and M. J. Lancaster, *Microstrip Filters for RF/Microwave Applications*. New York, NY, USA: Wiley, 2001.
[24] T. N. Kuo, S. C. Lin, C. H. Wang, and C. H. Chen, "New coupling scheme for microstrip bandpass filters with quarter-wavelength resonators," *IEEE Trans. Microw. Theory Techn.*, vol. 56, no. 12, pp. 2930–2935, Dec. 2008.
[25] D. M. Pozar, *Microwave Engineering*, 3rd ed. Hoboken, NJ, USA: Wiley, 2006.

CHI-FENG CHEN (M'12) was born in Pingtung, Taiwan, in 1979. He received the M.S. degree in electrophysics from National Chiao Tung University, Hsinchu, Taiwan, in 2003, and the Ph.D. degree in communication engineering from National Taiwan University, Taipei, Taiwan, in 2006.

From 2008 to 2010, he was an RF Engineer with Compal Communications, Inc., Taipei, Taiwan, where he developed global system for mobile communication (GSM) and code division multiple access (CDMA) mobile phones. In April 2010, he joined the Graduate Institute of Communication Engineering, National Taiwan University, as a Postdoctoral Research Fellow. Since 2012, he has been with the Department of Electrical Engineering, Tunghai University, Taichung, Taiwan, and became an Associate Professor, in 2016. His research interest includes the design of microwave circuits and associated RF modules for microwave and millimeter-wave applications.

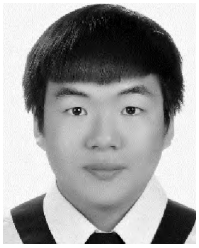

KAI-WEI ZHOU was born in Keelung, Taiwan, in 1996. He is currently pursuing the M.S. degree with the Department of Electrical Engineering, Tunghai University, Taichung, Taiwan. His current research interest includes the design of RF/microwave circuits.

RUEI-YI CHEN was born in Kaohsiung, Taiwan, in 1997. She is currently pursuing the M.S. degree with the Department of Electrical Engineering, Tunghai University, Taichung, Taiwan. Her current research interest includes the design of RF/microwave circuits.

ZU-CING WANG was born in Yilan, Taiwan, in 1997. She received the B.S. degree from the Department of Electrical Engineering, Tunghai University, Taichung, Taiwan, in 2019. Her current research interest includes the design of RF/microwave circuits.

YI-HUA HE was born in Taipei, Taiwan, in 1997. She is currently pursuing the M.S. degree with the Department of Electrical Engineering, Tunghai University, Taichung, Taiwan. Her current research interest includes the design of RF/microwave circuits.